Title	Joint stiffness contributes to hexapod gait stabilization
Author(s)	Nishii, Jun; Nagahori, Masayuki; Owaki, Dai
Citation	The 9.5th International Symposium on Adaptive Motion of Animals and Machines (AMAM2021). 2021, p. 41
Version Type	VoR
URL	https://doi.org/10.18910/84881
rights	
Note	

Joint stiffness contributes to hexapod gait stabilization

Jun Nishii[a], Masayuki Nagahori[a], Dai Owaki[b]
[a]Yamaguchi University, JAPAN
{nishii,i020vb}@yamaguchi-u.ac.jp
[b]Tohoku University, JAPAN
owaki@tohoku.ac.jp

1 Introduction

Although the morphology of insects varies among species, there are some typical features in their gait pattern [1]: (1) The contralateral leg moves in opposite phase, (2) The leg motion of the ipsilateral side shows a traveling wave propagating from back to front, and (3) Gait pattern changes from wave gait to tripod gait as walking speed increases. Many control models have been proposed to reproduce such a gait pattern [2, 3]; however, the role of elastic components of joints has not been discussed in such studies despite some studies suggesting its importance, especially in running animals [4, 5]. In the case of insects, muscles and exoskeleton contribute to elastic components, and the elastic force has been reported to contribute to the leg movements during walking [6]. The purpose of this study is to investigate how elastic components contribute to the gait generation of hexapod locomotion.

2 Methods

We prepared a hexapod model in which each leg has three links and joints (Fig. 1). For a control system, we used a reflex-based control model by Ekeberg and Pearson [7], which divides a stride cycle into four stages: stance, lift-off, swing, and touch-down. In each stage, constant torques were given to the 1st and 2nd (proximal and second proximal) joints. For the third (distal) joint, only passive torque by visco-elastic components was assigned. We also tested the locomotion performance under three conditions: (i) without and (ii) with visco-elastic components, and (iii) with foot pressure-dependent visco-elastic components at the 1st and 2nd joints. The transition between the stages was triggered by the proximal joint angle (from lift-off to swing and touch-down to stance) and foot pressure (from stance to lift-off and from swing to touch-down). The joint torque, thresholds of the transitions, and the viscoelastic coefficients were determined by the self-adaptive differential evolution (SADE) method [8] so as to minimize the cost of transport given by

$$E = \frac{1}{WD}\sum_{i=1}^{6}\sum_{j=1}^{2}\int_{0}^{T}(\delta(\tau_{ij}(t)\omega_{ij}(t)) + \gamma\tau_{ij}^{2}(t))dt$$

where W is the body weight, D is the linear distance traveled in the duration T, τ_{ij} and ω_{ij} are the joint torque and angular

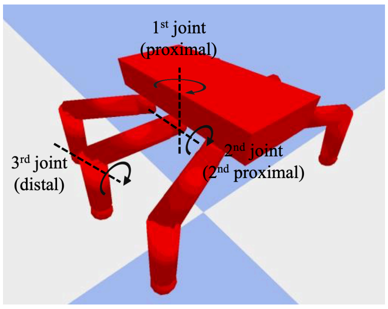

Figure 1: A hexapod model

velocity of the j-th joint of the i-th leg, respectively, $\delta(x)$ is the rectified linear unit, and $\gamma = 0.005$ is a constant that determines the maximum efficiency of the actuator [9].

The robot walked on level ground with no obstacles, and the cost of transport from 20 seconds to 80 seconds after the start of walking was used for evaluation. In the optimization computation by the SADE, the number of individuals in each generation was set to 100, and the optimization was performed up to 700 generations. In the simulation, Pybullet 3.05 was used, and the time step was set to 1/240 seconds.

3 Results and Discussion

When the 1st and 2nd joints have no visco-elastic components, the robot showed a non-periodic gait pattern (Fig. 2 (a)). When all joints were assigned visco-elastic components, the gait pattern was more periodic (Fig. 2 (b)); however, fluctuation of the gait was still observed and the leg movements showed only backward propagating waves. Fig. 3 (a) shows the time profile of the body pitch, roll, and yaw angles. The positive value of the pitch angle indicates that the robot is leaning backward.

In order to suppress the backward leaning, we added control of joint stiffness according to the foot pressure F in which the elastic and viscosity coefficients, k and σ, increase with F, i.e., $k = -(k_0 + aF)$, $\sigma = c(k_0 + aF)$, where k_0, a, and c are constants determined by the optimization computation. The result showed a more stable and periodic gait (Fig. 2(c)), and the robot exhibited forward and backward propagating waves alternately. When forward propagating waves were observed, the change in body sway was

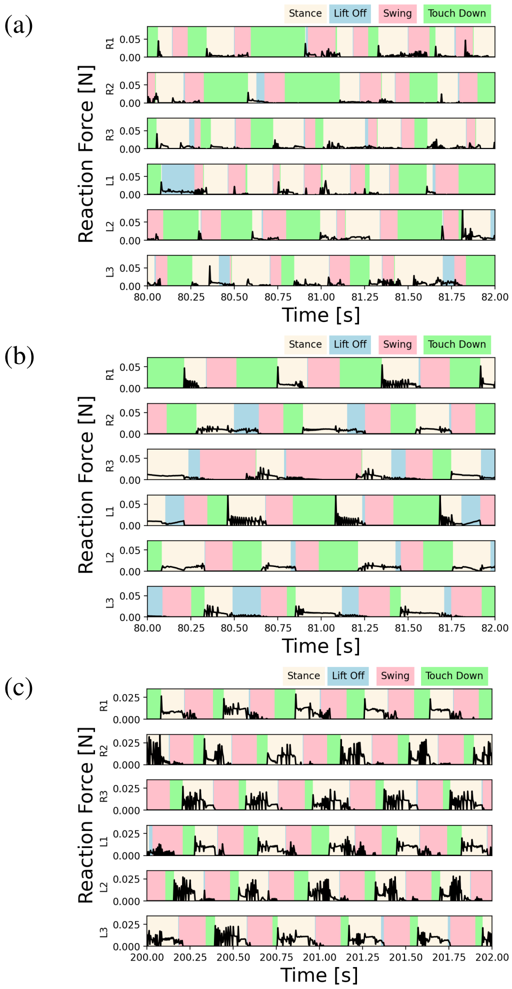

Figure 2: Gait diagram observed in the hexapod model with visco-elastic component at the 3rd joint (a) and all joints (b)(c). The subfigure (c) shows the result using foot-force dependent stiffness.

smaller (Fig.3 (b)(c)), and the cost of transportation was about 10% less.

4 Conclusion

In this study, we examined the gait pattern of a hexapod using a simple control model without inter-limb interaction. A periodic gait pattern with alternating forward and backward traveling waves emerged when all joints have visco-elastic components by which the joint stiffness changes with foot pressure. Although most previous studies have assumed some inter-limb interactions to obtain forward traveling wave [2, 3], our results showed that a simple control model produces it without such interactions. Our simulation results also showed that gait pattern with forward traveling wave suppresses body sway and the cost of transport. These results suggest that insects have developed a nervous system for inter-limb interaction to stabilize the forward traveling wave that realizes efficient locomotion through the evolutionary process.

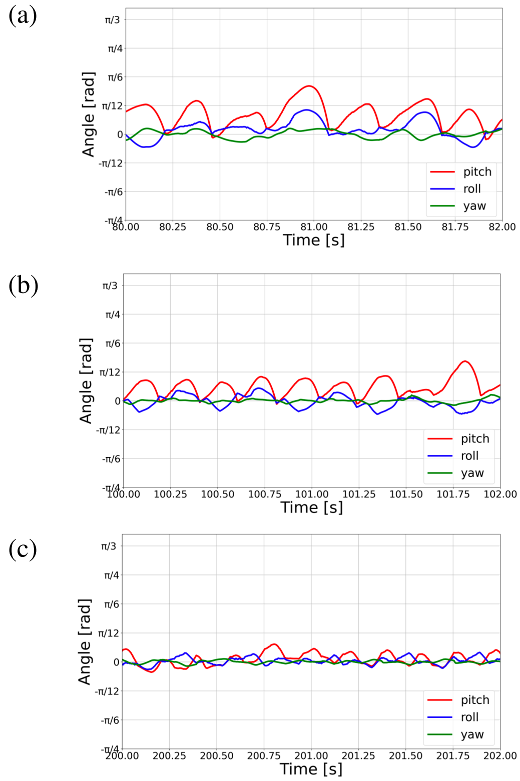

Figure 3: Time profile of the pitch, row, and yaw angles of the robot when all joints have visco-elastic components without (a) and with (b)(c) foot-force dependent stiffness. Subfigures (b) and (c) show the results when leg movements show backward and forward propagating wave, respectively.

5 Acknowledgements

We would like to thank Mr. Jonathan Arreguit at EPFL for his advice on optimization methods. This work was supported by JPSP KAKENHI Grant Number 18H03167.

References

[1] D.M. Wilson. Insect walking. *Annual Review of Entomology*, 11(1):103–122, 1966.

[2] H. Cruse, T. Kindermann, M. Schumm, J. Dean, and J. Schmitz. Walknet—a biologically inspired network to control six-legged walking. *Neural Networks*, 11(7-8):1435–1447, 1998.

[3] D. Owaki, M. Goda, S. Miyazawa, and A. Ishiguro. A minimal model describing hexapedal interlimb coordination: the tegotae-based approach. *Frontiers in Neurorobotics*, 11:29, 2017.

[4] R. Blickhan. The spring-mass model for running and hopping. *Journal of Biomechanics*, 22(11-12):1217–1227, 1989.

[5] C.T. Farley, H.H. Houdijk, Van Strien C., and M. Louie. Mechanism of leg stiffness adjustment for hopping on surfaces of different stiffnesses. *Journal of Applied Physiology*, 85(3):1044–1055, 1998.

[6] A. von Twickel, C. Guschlbauer, S.L. Hooper, and A. B.üschges. Swing velocity profiles of small limbs can arise from transient passive torques of the antagonist muscle alone. *Current Biology*, 29(1):1–12, 2019.

[7] O. Ekeberg and K. Pearson. Computer simulation of stepping in the hind legs of the cat: an examination of mechanisms regulating the stance-to-swing transition. *Journal of Neurophysiology*, 94(6):4256–4268, 2005.

[8] A.K. Qin and P.N. Suganthan. Self-adaptive differential evolution algorithm for numerical optimization. In *2005 IEEE Congress on Evolutionary Computation*, volume 2, pages 1785–1791. IEEE, 2005.

[9] J. Nishii. Legged insects select the optimal locomotor pattern based on the energetic cost. *Biological Cybernetics*, 83(5):435–442, 2000.